Computer Science and Information Systems 21(4):1745–1764 https://doi.org/10.2298/CSIS240314056C

# A Novel Image Enhancement Method Using Retinex-based Illumination Map Weighted Guided Filtering

Su Chen[1,⋆] and Dahai Li[2]

[1] Department of Mechanical and Electrical Engineering, Henan Vocational College of Water Conservancy and Environment
Zhengzhou 450002, China
chensssu@163.com

[2] School of Electronics and Electrical Engineering, Zhengzhou University of Science and Technology
Zhengzhou 450064, China
ldadahai@163.com

**Abstract.** Halo artifact, edge detail loss and noise amplification are the main problems in low illumination image enhancement, an image enhancement algorithm combining Retinex and illumination map weighted guided filtering is proposed. The traditional defogging physical models only enhance the images based on dark channels prior, resulting in different depths of field in local areas, and it can lead to some problems such as image overexposure and halo artifacts. To solve this problem, the method of combining light and dark channels is adopted to calculate the atmospheric light value and transmittance. For the problem that edge information is easily lost, the illumination gradient domain weighted guided filtering is utilized to improve the thinning transmittance. Experimental results with the proposed method have obvious improvement in denoising, halo elimination, brightness adjustment and edge preservation in the low-illumination image under different conditions.

**Keywords:** Image enhancement, Retinex, weighted guided filtering, dark channel.

## 1. Introduction

In the era of the information technology explosion, computer vision has played an increasingly important role in various fields. However, in the case where the light such as night or weak light is insufficient, the low-illumination type image has low contrast, low brightness, and detail information [1,2]. The imaging quality is seriously decreased, and the visual effect is poor, which is subsequently processed for the image and it has brought great challenges to a large extent to reduce computer vision applications [3-5]. Therefore, effective low illumination image enhancement has very important value in transportation and application prospects [6,7].

To perfect the demerits of low illumination images, the image enhancement algorithm must improve the image contrast, enhance the brightness, and highlight the details in the image. The current low illumination image enhancement methods mainly have the following categories.

⋆ Corresponding Author

1. Based on the histogram equalization algorithm, the histogram of distribution unevenness is evenly distributed by mapping changes, and the image contrast is improved. Based on this, scholars put forward a lot of improved algorithms such as contrast restricted adaptive histogram equilibrium, platform histogram equalization and adaptive platform histogram equalization [8,9], etc. When these algorithms heighten the low-illumination image overall, there is a problem that the high frequency grayscale affects low frequency grayscale or local enhancement.
2. Retinex-based algorithm, the reflection component characterized by the image is captured by removing the illumination component in the raw image. Zhuang et al. [10] combined Sigmod-MSR with original images for data loss issues. Kong et al. [11] presented a Retinex image enhancement approach based on Gauss-based bilateral filtering. Al-Hashim et al. [12] proposed a new way based on directional full variation Retinex for noise and artifacts. These algorithms can adjust the grayscale distribution of the image, but cannot improve the image detail, and easily produce color bias and color distortion.
3. The image-enhancement algorithms based on deep learning. Through a huge database training model, the input test image is processed, and a wide range of applications have been obtained in recent years. Liu et al. [13] combined attention mechanisms with convolutional neural networks (CNN) to remove brightness components in Retinex theory. Li et al. [14] designed a convolution with encoding and procrastics neural networks, constructing a generation and counteracting model to quickly complete image enhancement. These algorithms require a large number of data sets to train and test model, and the data set of the current low illumination images is limited. The synthesized low-illumination images and actual images are still different.
4. The degenerative physical model is built upon the atmospheric scattering model. In 2020, Liu et al., [15] found the similarity of low illumination images and fog days, and brought indirectly to low illumination image enhancement by combining the prior theoretical theory of dark channels (DCP). Because it had no sufficient constraint, there was an excessive or too small problem in the estimation of the transmittance and atmospheric light value, and the enhancement results often had a flare artifact. In response to these problems, Feng et al. [16] proposed a transmitting transmission rate in rapidly oriented filtering. Yu et al [17] proposed a binding super-resolution neural network with guided filter repelling fog. Mei et al. [18] showed a method of combining a brightness communication diagram with dark channels. Guo et al. [19] combined dark channels for super-poxes to correct atmospheric light value and transmittance. These modified algorithms have improved the estimation of atmospheric light values and transmittance to a certain extent, but there are still some problems such as indefinite edge, flare artifact and image exposure.

Image enhancement methods based on histogram equalization focus on adjusting the histogram distribution of input images to display more visual information. The histogram represents the distribution of pixel intensity in the image. When the overall image is dark, the histogram distribution can be equalized to adjust the contrast of the image. Lee et al. [20] proposed a contrast enhancement algorithm based on hierarchical difference of two-dimensional histograms to enhance image contrast by amplifying gray difference between adjacent pixels. Lin et al. [21] put forward a contrast enhancement algorithm that carried out color channel stretching, histogram averaging and remapping in sequence. By

stretching color channels, color information in the scene could be better restored, histogram averaging was re-equalized to enhance image content, and histogram remapping was used to reduce artifacts that often occurred in equalization. In order to better recover image content, Sujee et al. [22] combined the idea of multi-resolution with histogram equalization, used pyramid technology to decompose low-illumination images, and enhanced histogram matching for images with different resolutions to extract information from images to the maximum extent. Although the low-illumination image enhancement algorithm based on histogram equalization can enhance the contrast by simply stretching the dynamic range of the image gray scale, it does not consider the influence of ambient light, so this kind of algorithm will have the problem of over-enhancement or under-enhancement.

Retinex theory is a color constant theory, the main idea is that the color perceived by the human eye is determined by the joint action of the light reflected by the surface of the target object and the ambient illumination. According to Retinex theory, low illumination image is the combination of normal illumination image and environmental illumination, and the image of normal illumination can be obtained by removing the influence of environmental illumination in the image. How to separate the ambient illumination from the low-illumination image is a pathological problem, which is usually solved by some prior and constraint conditions. Chen et al. [23] proposed a multi-scale Retinex enhancement algorithm with color restoration, which combined dynamic range compression, color consistency and human visual stability to restore image brightness and contrast. Meng et al. [24] proposed an effective low-light image enhancement algorithm. First, the low-light image was inverted to make it visually close to the de-fogging image, then the de-fogging algorithm was used to process the image, and the enhanced image was inverted again. Yadav et al. [25] used the illuminance estimation algorithm based on morphological approximation to decompose the image into reflection component and illuminance component, and then carried out global brightness enhancement and local contrast enhancement operations on the illuminance component respectively. Finally, multi-scale fusion was used to obtain the illuminance image and obtain the image of normal illuminance. Zhou et al. [26] built the initial illuminance map by looking for the maximum value of image pixels in the three color channels of red, green and blue, and then used a predetermined structure to refine the initial illuminance map to obtain the final illuminance map and further achieved image illumination enhancement. Inspired by human vision, Li et al. [27] proposed a multi-stage multi-exposure image fusion framework. In the first stage, exposure was adjusted by simulating human eyes to generate multi-exposure image sets. The second stage simulated the human brain mechanism to fuse the multi-exposure images to obtain the final enhanced image. The key of low illumination image enhancement method based on Retinex model is the accuracy of illumination image estimation, which depends on the precise definition of prior constraints. However, a prior condition is difficult to apply to image enhancement of various real scenes.

Convolutional neural networks have strong feature learning ability, and have become the main tool to solve computer vision task problems, and are also widely used in low-illumination image enhancement tasks. Lore et al. [28] first proposed an image enhancement framework based on deep learning. By designing a depth autoencoder to identify the features of low-illumination images, image brightness could be adaptive enhanced, image enhancement and noise reduction could be realized at the same time. Li et al. [29]

proposed a decomposition network based on Retinex model. Firstly, the input image was decomposed into illuminance map and reflection map, then denoised and enhanced the illuminance map and reflection map respectively, and finally reconstructed two components to obtain the normal illuminance image. Wang et al. [30] regarded low-illumination image enhancement as a residual learning problem, that is, the image after brightness enhancement was obtained by estimating the residual difference between low-illumination image and normal illumination image. Xu et al. [31] proposed a brightness enhancement network based on frequency decomposition, which first restored the content information of the low frequency layer under the condition of suppressing noise, and then enhanced the details of the high frequency layer of the image. Zhang et al. [32] proposed a brightness enhancement network based on Retinex model decomposition, which designed a mapping function to flexibly adjust the brightness according to the different needs of users. The network also included an adjustment module, which could effectively remove the visual defects amplified by enhancing the brightness of darker areas.

In response to the above-mentioned enhancement algorithms and to restore the true color of the image, to solve the problem of image exposure, flare artifact and edge loss, etc., and to improve the visual effect of the image, we propose a dual-channel combining light gradient domain weighted guided filtering low illuminance image enhancement method. Images are acquired by some robot equipment. First, the bright channel is introduced, and the atmospheric light value is obtained by using a threshold method, and then the transmittance is obtained by the dual channel image pixel level. After Retinex decomposition, the optical illumination map is used as the guide map, and the multi-scale gradient domain weighted guide filter operation to refine the transmittance. The denoising optimization is performed using BM3D. Finally, it restores the image according to the dehazing physical model.

## 2. Related Works

This enhancement algorithm is based on the atmospheric scattering debris model with a priority theory of dark channels, which is the light map obtained by Retinex decomposing in image filtering. It obtains a final reinforcing image after comprehensive denoising optimization.

### 2.1. Atmospheric Scattering Physical Model

The fog degradation model is based on a classic atmosphere scattering model. The given input image $I$ to be removed from fog is:

$$I(x) = A\rho(x)exp[-\beta d(x)] + A(1 - exp[-\beta d(x)]). \tag{1}$$

Where $\rho(x)$ is density. $d(x)$ is the scene depth. $\beta$ is the scattering coefficient of the optical wavelength. $x$ is the pixel point position of the image. $A$ is a global atmospheric value. The first term on the right of formula (1) is the direct attenuation term, and the second term is the atmospheric light component. Let the transmission medium transmittance be $t(x) = exp[-\beta d(x)]$, the well-exposed natural images be $J(x) = A\rho(x)$, so the atmospheric scattering physical model is simplified as:

$$I(x) = J(x)t(x) + A[1 - t(x)]. \tag{2}$$

In reference [33], an improved atmospheric scattering model (IASM) was proposed to overcome the inherent limitation of the traditional atmospheric scattering model. Based on the IASM, a fast single image dehazing algorithm was also presented. In this algorithm, by constructing a linear model between the transmission and the haze aware density feature, the transmission map could be directly estimated through a linear operation on three components: luminance, saturation and gradient.

### 2.2. Dark Channel Prior and Bright Channel Prior

He et al. [34] obtained the dark channel prior theory through the statistics of 5000 outdoor fog-free images. In most non-sky local region images, there is at least one color channel with a very small intensity value approaching to zero. It is described as:

$$J_{dark}(x) = \min_{c \in R,G,B} \min_{x \in \Omega(x)} [J_c(x)] \to 0. \tag{3}$$

Where $J_{dark}$ is the dark primary color channel of the image. $J_c$ is the intensity of red (R), green (G) and blue (B) color channels of image $J$. $\Omega$ is the local area centered on pixel point $x$ with radius $r$.

The basic idea of bright channel prior is similar to dark channel prior. In most naturally sharp images, there is at least one color channel with a large intensity value approaching 255. It is described as:

$$J_{bright}(x) = \min_{c \in R,G,B} \max_{x \in \Omega(x)} [J_c(x)] \to 255. \tag{4}$$

Where $J_{bright}$ is the bright primary color channel of the image.

Reference [35] proposed a dual channel prior-based method for nighttime low illumination image enhancement with a single image, which built upon two existing image priors: dark channel prior and bright channel prior. It utilized the bright channel prior to get an initial transmission estimate and then used the dark channel as a complementary channel to correct potentially erroneous transmission estimates attained from the bright channel prior.

### 2.3. Retinex Theory

Retinex theory is also known as the retinal cortex theory [36]. According to this theory, the observed color information of an object is determined by the reflective nature of the object and the intensity of the surrounding light. The reflection property determines the intrinsic property of the image and the illumination part determines the dynamic range of the image pixel. Its mathematical model is:

$$I(x, y) = R(x, y) \times L(x, y). \tag{5}$$

Where $I(x, y)$ is the observed image. $R(x, y)$ is a reflection map. $L(x, y)$ is an illuminated map. This model can be referred to as a multiplication model, and only $R(x, y)$ can be decomposed from $I(x, y)$ to obtain a representation of the essence of the image.

In reference [37], different networks were first combined to construct a multi-branch module for features extraction, and used the module and Retinex theory to extract the reflection map of the image. Then an attention mechanism was introduced into the multi-branch construction to balance the feature weight of each branch, and get the final result by the reconstruction module. The Retinex theory was used to calculate the L1 loss and the gradient loss for the intermediate feature map of the entire model to train our framework.

## 3. Proposed Low-illuminance Enhancement Algorithm

The new algorithm first inverts the low-illumination image $I$, and then defogs the fog map. The light and dark channels of the image are obtained, and the initial atmospheric light $A_d$ and $A_b$ obtained by the two channels are combined to calculate the final atmospheric light value $A$. Through the dark-bright channel coefficients $t_d$ and $t_b$, combining with the dark-bright transmittance, the estimation of the initial transmittance $t$ is obtained. Illumination gradient domain weighted guided filtering (IGDWGIF) is used to refine and smooth the initial transmittance. Finally, the atmospheric scattering model is used to restore the original image. Then the obtained defogging image is inverted. The BM3D is used for denoising, and the final enhanced image $J$ is obtained. The flow chart is shown in figure 1.

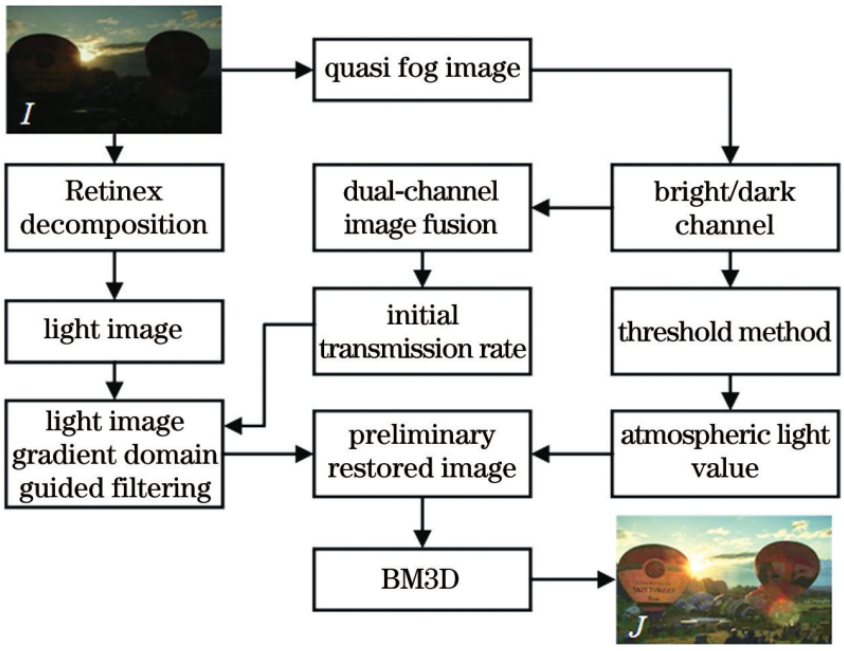


**Fig. 1.** The flow chart of the proposed low illumination enhancement algorithm

### 3.1. Threshold Method for Obtaining Atmospheric Light Value

For the calculation of global atmospheric light value A, if the brightest pixel of dark channel is directly used as atmospheric light value, there will be the problem of over-saturation. The atmospheric light value should be the radiation value at the depth of field infinity and the point should be in the background region of the image. Compared with the dark channel, the atmospheric light-dark density after merging with the bright channel is closer to the atmospheric light-dark density of the image to be enhanced. Therefore, the mean value of the pixel of the bright channel of the image to be enhanced can be used as the atmospheric light value. But some images completely contain sky or white objects, the results can be skewed.

To solve this problem, a threshold method is utilized to estimate atmospheric light value. Firstly, the light and shade profile of the image is judged, and the difference $I_{dif}$ between the bright channel $I_b$ and dark channel $I_d$ is calculated:

$$I_{dif} = I_b(x) - I_d(x). \tag{6}$$

For various types of low illumination images, the control variable method is used to conduct several enhancement experiments, and the threshold value $a$ is finally determined to be 0.38. If $I_{dif} > a$, it indicates that there is a large difference between the images of the two channels. Suspected points of atmospheric light with high pixel value are in the bright channel image. In order to avoid high values, the mean value of bright channel is used to estimate the atmospheric light value. If $I_{dif} \leq a$, it indicates that the suspected point of atmospheric light is on the dark object, and the atmospheric light value $a$ obtained only by using the bright channel prior is not reliable. For these unreliable pixels, $A_{cor}$ is obtained by combining dark channel prior images for correction, i.e,

$$A_{cor} = A_d \times A_b. \tag{7}$$

In summary, the atmospheric light value is:

$$A = \begin{cases} A_{bmean}, I_{dif} > a \\ A_{cor}, I_{dif} \leq a \end{cases} \tag{8}$$

Where $A_{bmean}$ is a mean value of bright channel.

Figure 2 shows the enhanced effect diagrams of atmospheric light values by different methods. It can be seen that the enhanced image obtained by the new method in this paper is clearer, and the addition of bright channels makes the details in the dark more obvious. The restoration at the lamp source is more natural, but there are still issues of halo and unclear edges, which will be solved by improving the transmittance.

### 3.2. Two-channel Estimated Transmittance

**Dark channel prior estimation of dark transmittance** According to equation (3), the image to be defogged after filtering and inverting is defogged. Minimum filtering is performed on both ends of equation (3) when atmospheric light value $A$ is known. It can obtain the following:

**Fig. 2.** Enhanced images of atmospheric light value via different methods. (a) Original image; (b) Reference [21]; (c) Proposed method

$$\min_{c\in R,G,B}\min_{x\in\Omega(x)} = t(x)\times\min_{c\in R,G,B}\min_{x\in\Omega(x)}[J_c(x)] + A_c[1-t(x)]. \tag{9}$$

Where $A_c$ is the atmospheric light value of any color channel. $I_c$ is any color channel of the image.

According to the dark channel prior theory, the dark channel of fog-free images tends to zero, so the first term on the right of equation (9) is 0. Meanwhile, in order to make the image look more natural and avoid excessive defogging, the defogging coefficient $m = 0.98$ is added to obtain the dark transmittance.

$$t_d(x) = 1 - m\times[\min_{c\in R,G,B}\min_{c\in R,G,B}[\frac{I_c(x)}{A_c}]]. \tag{10}$$

**Bright channel prior estimation of bright transmittance**

$$\max_{c\in R,G,B}\max_{x\in\Omega(x)}[I_c(x)] = t(x)\times\min_{c\in R,G,B}\min_{x\in\Omega(x)}[J_c(x)] + A_c[1-t(x)]. \tag{11}$$

According to the bright channel prior theory, the bright channel of fog-free images tends to 255. After image normalization, the pixel value of bright channel approaches to 1. The first term on the right of formula (11) is $t$, and the defogging coefficient $m$ is also added, so the transmittance is:

$$t_b(x) = m\times\frac{\max_{c\in R,G,B}\max_{c\in\Omega(x)} - A_c}{1-A_c}. \tag{12}$$

**Dual channel prior estimation of transmittance** Although the initial transmittance estimated by dark channel prior has achieved good results, not all images have dark channel. For some low illumination images with dark channel prior not tending to 0 (for example, when there is a large bright area), other auxiliary conditions are required. In addition, using only dark channel windows will lead to the coexistence of different depth-of-field in the same local area, which will lead to the wrong classification of pixel points at the junction of light and dark or at the junction of far and near scenes, resulting in the deviation of the estimation of transmittance. Therefore, the depth of field problem of the same local area can be corrected by adding bright channel prior and combining the local windows of both regions, so as to solve the halo artifact problem caused by transmittance estimation deviation. In this paper, the dark and bright channel coefficients $\alpha$ and $\gamma$ are used

to fuse the double channel, and then the transmittance is calculated. The enhancement effect can be better controlled by using certain linear relation. The specific relationship and constraint conditions are:

$$\begin{cases} t(x) = \alpha t_d(x) + \gamma t_b(x) \\ \alpha + \gamma = 1 \end{cases} \tag{13}$$

The transmittance will change as the values of $\alpha$ and $\gamma$ change. Experiments are carried out on Figure 2 under different $\alpha$ and $\gamma$ values. The experimental results are shown in Figure 3. It can be seen that the larger dark channel coefficient denotes the brighter transmittance image, the larger bright channel coefficient $\alpha$ and the darker transmittance image. When only dark channel is selected ($\alpha = 1$, $\gamma = 0$), there will be overexposure. When only the bright channel is selected ($\alpha = 10$, $\gamma = 1$), there will be a halo at the junction of the light, shade and the overall darkness. In order to make the overall light transparent and avoid overexposed, the effect is better when the dark channel coefficient is greater than the bright channel coefficient. Through a large number of low-illumination image enhancement experiments, the dark channel coefficient $\alpha$ is 0.75 and the bright channel coefficient $\gamma$ is 0.25.


**Fig. 3.** Transmittance images under different $\alpha$ and $\gamma$. (a) $\alpha = 1$, $\gamma = 0$; (b) $\alpha = 0.75$, $\gamma = 0.25$; (c) $\alpha = 0.25$, $\gamma = 0.75$; (d) $\alpha = 0$, $\gamma = 1$

### 3.3. Illumination Graph Multi-scale Gradient Weighted Guided Filtering (IGDWGIF)

Low illuminance image has a serious loss of detail, so it has higher requirements in detail preservation and edge preservation [38]. Guided filtering [39] (GIF) can not only smooth the image, but also has a better effect on edge detail preservation than bilateral filtering and other filters, with lower computational cost. On this basis, a series of improved algorithms are derived. Among them, multi-scale gradient-guided filtering (GDGIF) introduces clear edge constraints and adds image gradient information, resulting in clearer processing effects. The guiding image of the guiding filter is important in the filtering process. The guiding image has a variety of choices, which can be the image itself or other images. At present, the image enhancement field uses a wide range of grayscale images to be enhanced, dark channel images, and RGB images to be enhanced. Good guided images make filtering results more structural.

Formula (1) is deformed so that $t(x) = exp[-\beta d(x)]$, and it can obtain:

$$1 - \frac{I(x)}{A} = t(x)[1 - \rho(x)]. \tag{14}$$

Defining $M(x) = 1 - \frac{I(x)}{A}$, $N(x) = 1 - \rho(x)$, it can obtain:

$$M(x) = t(x)N(x). \tag{15}$$

Where $N(x)$ is the inverse albedo. Formula (15) is defined as the multiplication model, which simply separates $t(x)$ and $N(x)$ from $M(x)$. This model is similar to Retinex algorithm. Retinex uses the filtering to decompose the light and reflection images. Here, illumination graph L is continuous and smooth in space. The transmittance $t(x)$ is a continuous function of depth and also remains smooth in space. They have similar properties. R is a reflection graph, which has the characteristics of large local variation and is similar to the inverse albedo $N(x)$. Based on this, this paper proposes a new guided filter, that is, illumination map multi-scale gradient weighted guided filter. Figure 4 is the edge information extraction images with different guidance graphs. Table 1 shows the similarity comparison between the original image and different guided images.

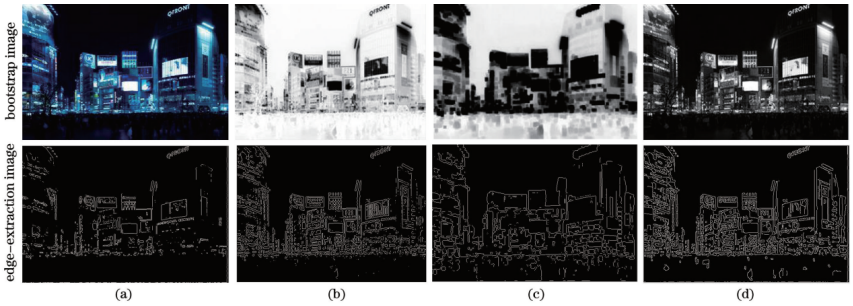


**Fig. 4.** Edge extraction images with different guided images (a) Original image (b) Gray-level inversion image (c) Dark-channel image (d) Illumination image

**Table 1.** Similarity between different guided images and original images

| Guided image | Similarity |
|---|---|
| Gray-level inversion | 0.2061 |
| Illumination image | 0.5677 |
| Dark-channel | 0.4052 |

In Figure 4, when the guided image adopts the image itself, filtering becomes an operation that only preserves edge and loses part of edge information. The gray scale inverse image is the pseudo fog image of low illuminance image under dark channel prior algorithm. Compared with the original image, the pixel value is higher, and the value is more than 200. In the chroma channel processing of the subsequent resulting image, the available edge details and brightness information are deviated, which makes the enhanced image overexposed and affects the color of the final enhanced image. When the guided image is used as a dark channel image, the pixel value is also high or low,

and the filtered image is blocky, so the details need to be improved. As a guided image, brightness image is better than gray image and dark channel image in both brightness and edge extraction. Compared with the original image, the brightness information of the image is richer and more consistent with the color characteristics of the object itself. It avoids too high brightness to affect the reduction effect. It enhances the detail information of dark area to some extent and is beneficial to image restoration.

From $t(x) = exp[-\beta d(x)]$, we can know that the transmittance $t$ is a continuous function of depth of field $d$ and concentration $\beta$. Dark channel prior is valid only when $t \to 1$. That is, when $\beta$ is large, the prior condition is satisfied with $d \to 0$, otherwise, it is not. In order to make the vision also meet the prior conditions, the value of concentration $\beta$ can be reduced and the method of two-time selective filtering can be adopted. That is, the concentration $\beta$ is gradually reduced so that the prospect also satisfies the conditions of the prior theory. In summary, combining the properties of multi-scale gradient weighted guided filtering and brightness image, IGDWGIF enables the filtered image to better restore the low-illuminance image in terms of gradient information, texture information and color information.

### 3.4. Image Denoising Optimization Based on BM3D

Low illumination images generally have the problem of excessive noise, which has a great influence on image enhancement. Therefore, it is necessary to optimize the image denoising [40-43]. Through many experiments, if the denoising stage is carried out before enhancement, the original dark image will become more blurred and the image details will also be affected. Therefore, the optimization step of denoising is executed at the end of the algorithm, so as to achieve the purpose of optimizing and enhancing the image.

Most of the noise in low illuminance images are Gaussian noise generated during transmission and Poisson noise generated under low illuminance. Among them, the latter accounts for the majority. Therefore, block-matching and 3D filtering (BM3D) [44] is adopted for denoising. The BM3D mainly includes basic estimation and final denoising. The similarity block with the least difference [45] in the image is found and integrated into a three-dimensional matrix, which is transformed into a two-dimensional matrix to obtain the basic estimation. The denoising image is obtained by weighted average of the repeated values after filtering. When BM3D searches for reference pixel blocks, the step size is 4 pixel, and the complexity is reduced to 1/16 of that when the step size is 1, effectively shortening the computing time.

Here we conduct image denoising experiments with two methods BM3D and TWSC [46] to show the robust of BM3D. Result is shown in figure 5. The Gaussian noise is set to 35. In Figure 5, we find that at such a high noise level, the observed image is heavily degraded and many significant details are lost. SRR-A can effectively remove noise, but it causes the restored image to be over-smoothed and many significant details are lost. The image restored by BM3D has the most details and best overall appearance.

## 4. Experiments and Analysis

Here, 500 low-illuminance images are collected in this paper, including low-illuminance images at night. In this paper, three different enhancement models are selected to compare with the proposed method including NCTV [47], RFA [48] and FFTR [49].

(a) (b) (c)

**Fig. 5.** Experimental results with BM3D and TWSC. (a) Noisy image;(b) TWSC; (c) BM3D

### 4.1. Low Illumination Images with a Large Sky Area and a Wide Variation in Depth of Field

Low illumination image enhancement [50] with a large sky area and large variation of depth of field has always been one of the difficulties in research. The enhancement results of these images are compared and analyzed from two aspects: subjective evaluation and objective evaluation. The results are shown in Figure 6.

As can be seen from Figure 6(b1)-(b4), the enhancement results of the NCTV have halo artifacts. The white object is particularly obvious around, the contour of the restored object is not clear enough, and the overall image is dark. As shown in Figure 6(b2) and (b3), obvious halo can be seen, and the objects on the left side of the building in Figure 6(b1) and the hot air balloon on the ground in Figure 6(b4) are blurred with serious loss of details. As can be seen from Figure 6(cl)-(c4), the image brightness and contrast of the RFA are significantly improved compared with the NCTV algorithm. However, there is a certain over-exposure phenomenon, which is reflected in the sky region in Figure 6(c2) and Figure 6(c3). In Figure 6(c3), the boundary between the cloud and the sky is not obvious, and the circular corridor information of the object is lost. From Figure 6(d1)-(d4), it can be seen that the overall enhancement effect of the FFTR is relatively natural, and both brightness and contrast are improved. However, there is a certain color deviation phenomenon, especially in the building part of 6(d3) and the sky area of Figure 6(d4), the color distortion is obvious. The proposed algorithm gives more accurate estimations for atmospheric light value and transmittance. Therefore, it has a good effect in enhancing brightness and contrast and restoring sky region, as shown in Figure 6(e1)-(e4). The edge of the object is clear, the details are rich, there is no color distortion and halo phenomenon, the overall enhancement effect is more natural and clear. The visual effect is obviously better than other algorithms.

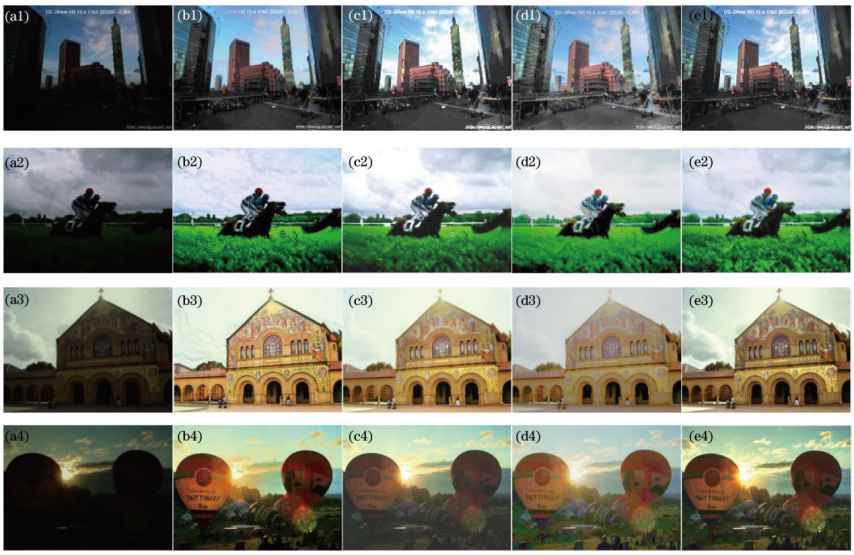


**Fig. 6.** Enhancement results of low-illumination images with large sky areas and obvious change in depth of field for different methods. (a1)-(a4) Original images; (b1)-(b4) NCTV method; (c1)-(c4) RFA method; (d1)-(d4) FFTR method; (e1)-(e4) proposed method

### 4.2. Low Illuminance Images with Light Source and Uneven Light

In the process of low illumination image enhancement with light source and non-uniform light, halo artifacts often appear. The enhancement results of such images are also compared, and the experimental results are shown in Figure 7.

As can be seen from Figure 7(b1)-(b3), no matter in indoor or outdoor light source, the enhancement results of the NCTV all have obvious halo phenomenon and the overall image is dark. In Figure 7(b1) and Figure 7(b3), the halo phenomenon can be clearly seen at the light source. In Figure 7(b2), the restoration of some small objects in the book is not clear enough, and a lot of image information is lost. The RFA algorithm is better than the NCTV in detail enhancement and halo artifact removal. However, obvious overexposure still exists in the light source and white objects, as reflected in the light in Figure 7(c1) and white objects in Figure 7(c2). The FFTR algorithm has good halo removal effect and dark area detail reduction effect in light source or white object, but there is color skew phenomenon and the overall color is lighter. As shown in Figure 7(d2), the restoration of dark area background is more complete with more details. However, the enhanced results of Figure 7(d1)-(d3) all have different degrees of color distortion. By combining dual channel and illumination guided filtering, the overall effect of the proposed algorithm is better than the previous algorithms in image restoration. As shown in Figure 7(e1) and Figure 7(e3), the enhancement at the light source is more natural. The image detail restoration in Figure 7(e2) is richer and more comprehensive, and the texture details of the image are clearer and the visual effect is better.


**Fig. 7.** Enhancement results of low-illumination images with light source and inhomogeneous light images with different methods. (a1)-(a3) Original images; (b1) (b3) NCTV method; (c1)-(c3) RFA method; (d1)-(d3) FFTR method; (e1)-(e3) proposed method

In order to compare the effect of low illumination image enhancement algorithm objectively and fairly, the evaluation indexes of image information entropy, average gradient and structure similarity are selected for comparative analysis.

Image information entropy represents the richness of image information. The higher entropy of image information denotes the image containing more information, and the richer image. It is represented as:

$$H = -\sum_{x=0}^{255} p_x lbp_x. \tag{16}$$

Where $p_x$ is the occurrence probability of pixel point $x$. As shown in Table 2 (figure 8 is the visible result), the algorithm in this paper has a better overall effect and can make the enhanced image contain richer information. Moreover, the enhancement effect is natural and clear, and the color fidelity is better, which is consistent with subjective evaluation.

**Table 2.** Information entropy comparison

| Original image | NCTV | RFA | FFTR | Proposed |
|---|---|---|---|---|
| Figure 6(a1) | 7.3627 | 7.7676 | 7.6044 | 7.9873 |
| Figure 6(a2) | 6.8835 | 7.1563 | 7.2614 | 7.5858 |
| Figure 6(a3) | 7.6608 | 7.6252 | 7.2637 | 7.9068 |
| Figure 6(a4) | 6.9669 | 7.6201 | 7.2637 | 7.6299 |
| Figure 7(a1) | 6.4774 | 7.0699 | 7.1874 | 7.2673 |
| Figure 7(a2) | 5.6373 | 6.3463 | 6.3542 | 6.8835 |
| Figure 7(a3) | 6.1473 | 6.9075 | 6.8736 | 7.1347 |

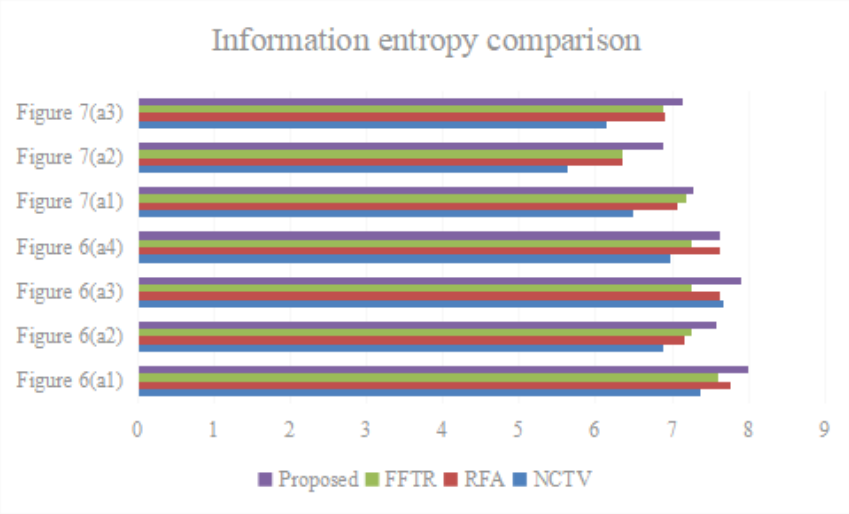


**Fig. 8.** Visualized result of Table 2.

The average gradient represents the detail information of the image. The larger average gradient denotes the clearer contour of the image and the richer detail information. It is represented as:

$$A = \frac{\sum_{i=1}^{w-1}\sum_{j=1}^{n-1}\sqrt{\frac{(J_{i,j}-J_{i+1,j})^2+(J_{i,j}-J_{i,j+1})^2}{2}}}{(w-1)(n-1)}. \tag{17}$$

Where $J_{i,j}$ is the pixel value of the $i-th$ row and $j-th$ column of the image matrix. $w$ and $n$ are the number of rows and columns of the image matrix respectively. As shown in Table 3 (figure 9 is the visible result), the average image gradient of the proposed algorithm is slightly lower than that of RFA in Figure 6(a1), and the overall average gradient performance is good. It can well maintain edges and restore details, enhance the image hierarchies, which is consistent with subjective evaluation.

**Table 3.** Average gradient comparison

| Original image | NCTV | RFA | FFTR | Proposed |
|---|---|---|---|---|
| Figure 6(a1) | 9.0718 | 11.9962 | 9.8472 | 10.1511 |
| Figure 6(a2) | 6.9855 | 6.5608 | 5.1720 | 9.0468 |
| Figure 6(a3) | 4.3488 | 5.4321 | 4.1092 | 6.3789 |
| Figure 6(a4) | 2.3238 | 2.2982 | 2.9927 | 3.2041 |
| Figure 7(a1) | 5.3746 | 6.9806 | 6.3413 | 7.1136 |
| Figure 7(a2) | 3.3274 | 5.8399 | 4.4367 | 5.9964 |
| Figure 7(a3) | 7.1267 | 7.9746 | 7.3422 | 8.3473 |

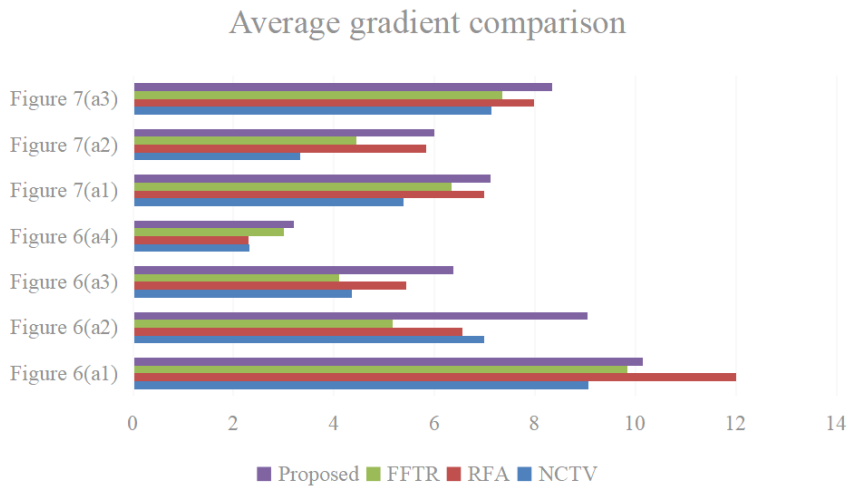


**Fig. 9.** Visualized result of table 3.

Structural similarity represents the similarity of content structure before and after image restoration. The value is close to 1, the quality of enhanced image is better. It is represented as:

$$S(X,Y) = \frac{(2\mu_X\mu_Y)(\sigma_{XY} + C_2)}{(\mu_X^2\mu_Y^2 + C_1)(\sigma_X^2 + \sigma_Y^2 + C_2)}. \tag{18}$$

Where $S(X,Y)$ is structural similarity. $\mu_X$ and $\mu_Y$ are the mean values of images $X$ and $Y$ respectively. $\sigma_X$ and $\sigma_Y$ are the standard deviations of image $X$ and $Y$ respectively. $\sigma_{XY}$ is the covariance of images $X$ and $Y$. $C_1$ and $C_2$ are constants. As shown in Table 4 (figure 10 is the visible result), the structure similarity of the proposed algorithm is closest to 1, and the image texture is clear without redundant halo artifacts and noise amplification.

**Table 4.** Structural similarity comparison

| Original image | NCTV | RFA | FFTR | Proposed |
|---|---|---|---|---|
| Figure 6(a1) | 0.6314 | 0.7046 | 0.6099 | 0.7344 |
| Figure 6(a2) | 0.5143 | 0.6322 | 0.5321 | 0.6945 |
| Figure 6(a3) | 0.7097 | 0.7636 | 0.6625 | 0.8069 |
| Figure 6(a4) | 0.6354 | 0.8093 | 0.7312 | 0.8144 |
| Figure 7(a1) | 0.6833 | 0.6919 | 0.5281 | 0.7221 |
| Figure 7(a2) | 0.6707 | 0.6228 | 0.5871 | 0.6974 |
| Figure 7(a3) | 0.5314 | 0.6372 | 0.4145 | 0.6738 |

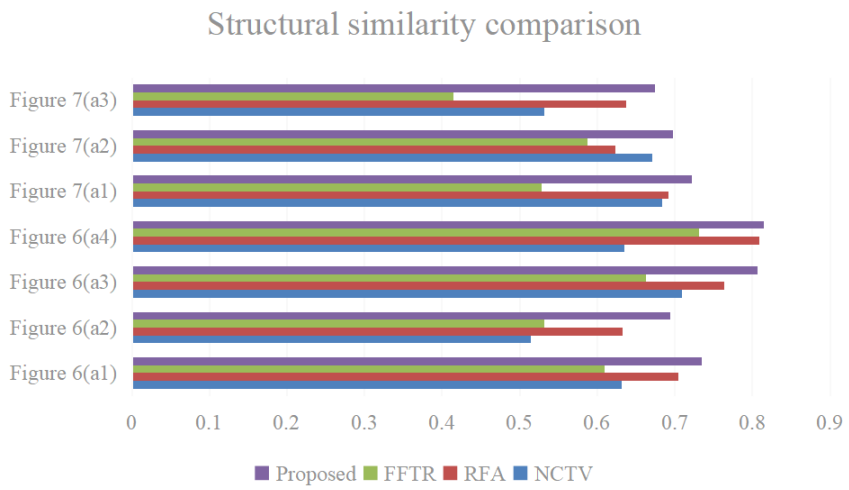


**Fig. 10.** Visualized result of table 4.

## 5. Conclusion

Aiming at the problems of halo artifact, brightness oversaturation, edge detail loss and noise amplification in the process of low illumination image enhancement by defogging physical model, an image enhancement method combining dual-channel prior and illumination gradient domain weighted guided filtering was proposed. The atmospheric light value is obtained by introducing broad value method of bright channel image, and the light channel priors are fused with dark channel priors to obtain the initial transmittance. The transmittance is refined by weighted guided filtering in illumination gradient domain. BM3D optimization denoising method is used to enhance the image, which solves the problem that dark channel prior is not suitable for the large bright areas and the same local area has different depth of field, making the estimation of atmospheric light value and transmittance more accurate. Results show that the new algorithm has obvious improvement in halo elimination, brightness adjustment, edge preservation and noise removal. Although many new methods have been proposed, in the future, we will use the most advanced deep learning methods to enhance images, in order to apply them to practical engineering applications.

## References

1. He L, Long W, Liu S, et al. A night low-illumination image enhancement model based on small probability area filtering and lossless mapping enhancement[J]. IET Image Processing, 2021, 15(13): 3221-3238.
2. Che Aminudin M F, Suandi S A. Video surveillance image enhancement via a convolutional neural network and stacked denoising autoencoder[J]. Neural Computing and Applications, 2022: 1-17.
3. Wang X. Crowd density estimation based On multi-scale information fusion And matching network in scenic spots[J]. Journal of Applied Science and Engineering, 2022, 26(6): 863-873.

4. Wang J, Yang Y, Chen Y, et al. (2021) LighterGAN: An Illumination Enhancement Method for Urban UAV Imagery[J]. Remote Sensing, 13(7): 1371.
5. Shen W. (2022) A Novel Conditional Generative Adversarial Network Based On Graph Attention Network For Moving Image Denoising[J]. Journal of Applied Science and Engineering, 26(6): 831-841.
6. L. Bai, W. Zhang, X. Pan and C. Zhao, (2020) "Underwater Image Enhancement Based on Global and Local Equalization of Histogram and Dual-Image Multi-Scale Fusion," in IEEE Access, vol. 8, pp. 128973-128990, doi: 10.1109/ACCESS.2020.3009161.
7. Peng Y, Wang W, Tang Z, et al. (2022) Non-uniform illumination image enhancement for surface damage detection of wind turbine blades[J]. Mechanical Systems and Signal Processing, 170: 108797.
8. N. H. Saad, N. A. M. Isa and H. M. Saleh, (2021) "Nonlinear Exposure Intensity Based Modification Histogram Equalization for Non-Uniform Illumination Image Enhancement," in IEEE Access, vol. 9, pp. 93033-93061, doi: 10.1109/ACCESS.2021.3092643.
9. Liu S, Long W, He L, et al. Retinex-based fast algorithm for low-light image enhancement[J]. Entropy, 2021, 23(6): 746.
10. Zhuang P, Li C, Wu J. (2021) Bayesian retinex underwater image enhancement[J]. Engineering Applications of Artificial Intelligence, 101(1):104171.
11. X. -Y. Kong, L. Liu and Y. -S. Qian, (2021) "Low-Light Image Enhancement via Poisson Noise Aware Retinex Model," in IEEE Signal Processing Letters, vol. 28, pp. 1540-1544, doi: 10.1109/LSP.2021.3096160.
12. Al-Hashim M A, Al-Ameen Z. (2020) Retinex-Based Multiphase Algorithm for Low-Light Image Enhancement[J]. Traitement du Signal, 37(5):733-743.
13. Liu K, Tian Y. (2020) Research and analysis of deep learning image enhancement algorithm based on fractional differential[J]. Chaos, Solitons & Fractals, 131.
14. Li G, Yang Y, Qu X, et al. (2021) A deep learning based image enhancement approach for autonomous driving at night[J]. Knowledge-Based Systems, 213: 106617.
15. X Liu, Gao Z, Chen B M. (2020) IPMGAN: Integrating physical model and generative adversarial network for underwater image enhancement[J]. Neurocomputing, 453(3).
16. Feng X, J Li, Hua Z. (2020) Low-light image enhancement algorithm based on an atmospheric physical model[J]. Multimedia Tools and Applications, 79(3).
17. S. Yu and H. Zhu, (2019) "Low-Illumination Image Enhancement Algorithm Based on a Physical Lighting Model," in IEEE Transactions on Circuits and Systems for Video Technology, vol. 29, no. 1, pp. 28-37, doi: 10.1109/TCSVT.2017.2763180.
18. Y. Mei and Y. Ning, (2019) "Multilayer Fusion and Chunk-Based Transmittance Estimation for Natural Hazy Image Enhancement," in IEEE Access, vol. 7, pp. 118269-118277, doi: 10.1109/ACCESS.2019.2937111.
19. Guo J, Li C, Guo C, et al. (2017) Research progress of underwater image enhancement and restoration methods[J]. Journal of Image and Graphics, 22(3), 273-287.
20. Lee C, Lee C, Kim C S. Contrast enhancement based on layered difference representation of 2D histograms[J]. IEEE transactions on image processing, 2013, 22(12): 5372-5384.
21. Lin S C F, Wong C Y, Rahman M A, et al. Image enhancement using the averaging histogram equalization (AVHEQ) approach for contrast improvement and brightness preservation[J]. Computers & Electrical Engineering, 2015, 46: 356-370.
22. Sujee R, Padmavathi S. Image enhancement through pyramid histogram matching[C]//2017 International Conference on Computer Communication and Informatics (ICCCI). IEEE, 2017: 1-5.
23. Chen B, Zhu L, Zhu H, et al. Gap-Closing Matters: Perceptual Quality Evaluation and Optimization of Low-Light Image Enhancement[J]. IEEE Transactions on Multimedia, 2023.
24. Meng X, Huang J, Li Z, et al. DedustGAN: Unpaired learning for image dedusting based on Retinex with GANs[J]. Expert Systems with Applications, 2024, 243: 122844.

25. Yadav G, Yadav D K, Mouli P C. Fusion-based backlit image enhancement and analysis of results using contrast measure and SSIM[M]//Digital Image Enhancement and Reconstruction. Academic Press, 2023: 235-251.
26. Zhou J, Liu Q, Jiang Q, et al. Underwater camera: Improving visual perception via adaptive dark pixel prior and color correction[J]. International Journal of Computer Vision, 2023: 1-19.
27. Li H, Wu X J. CrossFuse: A novel cross attention mechanism based infrared and visible image fusion approach[J]. Information Fusion, 2024, 103: 102147.
28. Lore K G, Akintayo A, Sarkar S. LLNet: A deep autoencoder approach to natural low-light image enhancement[J]. Pattern Recognition, 2017, 61: 650-662.
29. Li J, Hao S, Li T, et al. RDMA: low-light image enhancement based on retinex decomposition and multi-scale adjustment[J]. International Journal of Machine Learning and Cybernetics, 2023: 1-17.
30. Wang L W, Liu Z S, Siu W C, et al. Lightening network for low-light image enhancement[J]. IEEE Transactions on Image Processing, 2020, 29: 7984-7996.
31. Xu K, Yang X, Yin B, et al. Learning to restore low-light images via decomposition-and-enhancement[C]//Proceedings of the IEEE/CVF conference on computer vision and pattern recognition. 2020: 2281-2290.
32. Zhang Y, Zhang J, Guo X. Kindling the darkness: A practical low-light image enhancer[C]//Proceedings of the 27th ACM international conference on multimedia. 2019: 1632-1640.
33. Ju M, Gu Z, Zhang D. (2017) Single image haze removal based on the improved atmospheric scattering model[J]. Neurocomputing, 260: 180-191.
34. K. He, J. Sun and X. Tang, (2011) "Single Image Haze Removal Using Dark Channel Prior," in IEEE Transactions on Pattern Analysis and Machine Intelligence, vol. 33, no. 12, pp. 2341-2353, doi: 10.1109/TPAMI.2010.168.
35. Shi Z, Guo B, Zhao M, et al. (2018) Nighttime low illumination image enhancement with single image using bright/dark channel prior[J]. EURASIP Journal on Image and Video Processing, 2018(1): 1-15.
36. Jung C, Tian S, Jiao L. (2013) Eye detection under varying illumination using the retinex theory[J]. Neurocomputing, 113(aug.3):130-137.
37. Li M, Zhou D, Nie R, et al. (2021) AMBCR: Low-light image enhancement via attention guided multi-branch construction and Retinex theory[J]. IET Image Processing, 15(9): 2020-2038.
38. Wang, H., Su, Z., Liang, S. (2019). Structure-Preserving Guided Image Filtering. Intelligence Science and Big Data Engineering. Visual Data Engineering. IScIDE 2019. Lecture Notes in Computer Science, vol. 11935. Springer, Cham.
39. Wang L, Shoulin Y, Alyami H, et al. A novel deep learning-based single shot multibox detector model for object detection in optical remote sensing images[J]. Geoscience Data Journal, 2022. https://doi.org/10.1002/gdj3.162.
40. Feng D, Li T, Li G, et al. (2022) Reverse time migration of GPR data based on accurate velocity estimation and artifacts removal using total variation de-noising[J]. Journal of Applied Geophysics, 198:104563-.
41. Wei D. (2021) Retinex-Based Fast Algorithm for Low-Light Image Enhancement[J]. Entropy, 23.
42. Pan X, Li C, Pan Z, et al. (2022) Low-Light Image Enhancement Method Based on Retinex Theory by Improving Illumination Map[J]. Applied Sciences, 12(10): 5257.
43. Lu B, Pang Z, Gu Y, et al. (2022) Channel splitting attention network for low-light image enhancement[J]. IET Image Processing, 16.
44. K. Dabov, A. Foi, V. Katkovnik and K. Egiazarian, (2007) "Image Denoising by Sparse 3-D Transform-Domain Collaborative Filtering," in IEEE Transactions on Image Processing, vol. 16, no. 8, pp. 2080-2095, doi: 10.1109/TIP.2007.901238.
45. Zhang J, Wei Z. (2021) Image Enhancement Algorithm for Low Illumination LCD Screen[J]. Frontiers in Science and Engineering, 1(1): 1-8.

46. Xu J, Zhang L, Zhang D. (2018) A trilateral weighted sparse coding scheme for real-world image denoising[C]//Proceedings of the European conference on computer vision (ECCV). 20-36.
47. Kang M, Jung M. Simultaneous image enhancement and restoration with non-convex total variation[J]. Journal of Scientific Computing, 2021, 87(3): 83.
48. Xu Y, Sun B. (2022) A Novel Variational Model for Detail-Preserving Low-Illumination Image Enhancement[J]. Signal Processing, 195:108468-.
49. Kaur K, Jindal N, Singh K. Fractional Fourier Transform based Riesz fractional derivative approach for edge detection and its application in image enhancement[J]. Signal Processing, 2021, 180: 107852.
50. Yin S, Li H, Sun Y, et al. Data Visualization Analysis Based on Explainable Artificial Intelligence: A Survey[J]. IJLAI Transactions on Science and Engineering, 2024, 2(2): 13-20.

**Su Chen** female, Han nationality, born in Zhengzhou, Henan Province, Master, Lecturer, Mechanical and Electrical Engineering Department, Henan Vocational College of Water Conservancy and Environment, research interests: automatic control, image processing.

**Dahai Li** male, Han nationality, born in Zhengzhou, Henan Province, Master, Associate Professor, School of Electronics and Electrical Engineering, Zhengzhou University of Science and Technology, research interests: embedded technology development, image processing.

*Received: March 14, 2024; Accepted: June 29, 2024.*